Science Advances
AAAS

advances.sciencemag.org/cgi/content/full/4/11/eaat4388/DC1

Supplementary Materials for

A swarm of slippery micropropellers penetrates the vitreous body of the eye

Zhiguang Wu, Jonas Troll, Hyeon-Ho Jeong, Qiang Wei, Marius Stang, Focke Ziemssen, Zegao Wang, Mingdong Dong, Sven Schnichels, Tian Qiu*, Peer Fischer*

*Corresponding author. Email: qiu@is.mpg.de (T.Q.); fischer@is.mpg.de (P.F.)

Published 2 November 2018, *Sci. Adv.* **4**, eaat4388 (2018)
DOI: 10.1126/sciadv.aat4388

The PDF file includes:

Other Supplementary Material for this manuscript includes the following:

(available at advances.sciencemag.org/cgi/content/full/4/11/eaat4388/DC1)

Movie S1 (.avi format). Wobbling motion of an uncoated micropropeller in the vitreous under the actuation of a rotating magnetic field with a strength of 8 mT and a frequency of 6 Hz.

Movie S2 (.avi format). Propulsion of a slippery micropropeller in the vitreous under the actuation of a rotating magnetic field with a strength of 8 mT and a frequency of 6 Hz.
Movie S3 (.avi format). A large swarm of slippery micropropellers moves across the boundary of an aqueous buffer into the vitreous and continues propelling in the vitreous under a rotating magnetic field with a strength of 8 mT and a frequency of 70 Hz.
Movie S4 (.avi format). Controlled motion of slippery micropropellers in the vitreous under a rotating magnetic field with a strength of 8 mT and a frequency of 50 Hz.
Movie S5 (.avi format). OCT shows the distribution of the slippery micropropellers at the vitreous-retina boundary.

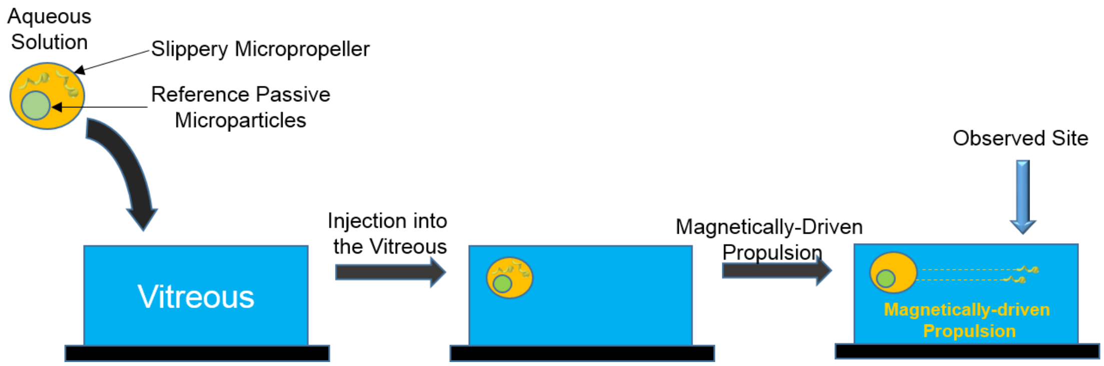

Fig. S1. Schematic of the experimental scheme used to confirm the movement of the propellers in the vitreous. The observed site is 3 mm away from the initial injection spot.

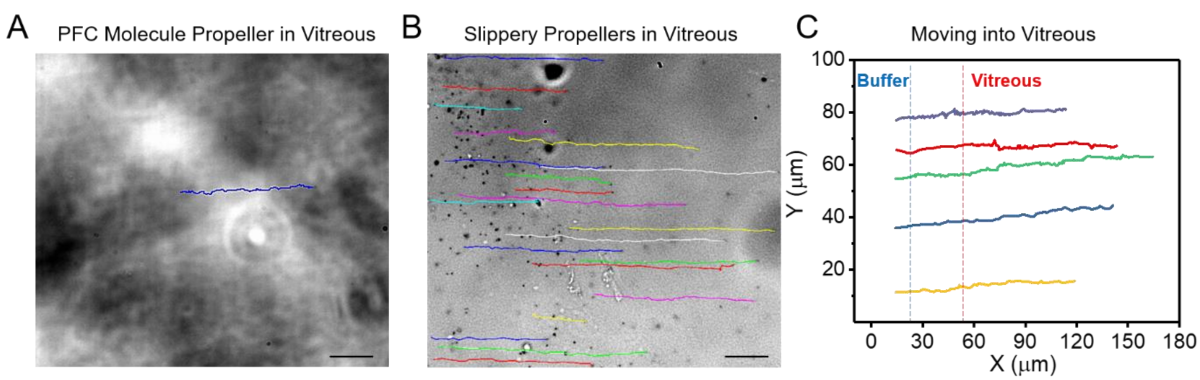

Fig. S2. Intravitreal propulsion of micropropellers with different coatings. (**A**) Microscope image shows that only a few of the perfluorocarbon molecule-only-functionalized micropropellers are able to move in the vitreous (tracked trajectory in blue). (**B**) Microscope image shows that a large swarm of the liquid-coated slippery micropropellers moves cross the boundary of the buffer into the vitreous and continuously inside the vitreous. Colored lines indicate the trajectories of the micropropellers. (**C**) The trajectory of the micropropeller propelling from the buffer solution to the vitreous. Scale bar 20 μm.

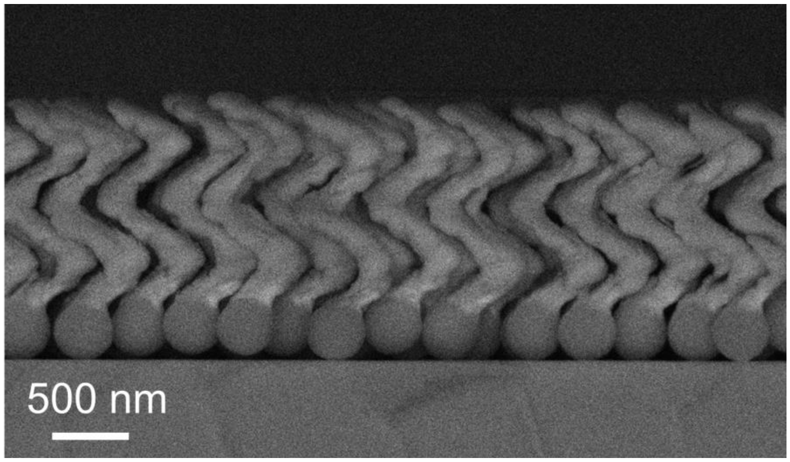

Fig. S3. SEM images of the micropropellers grown with TiO_2 and Fe.

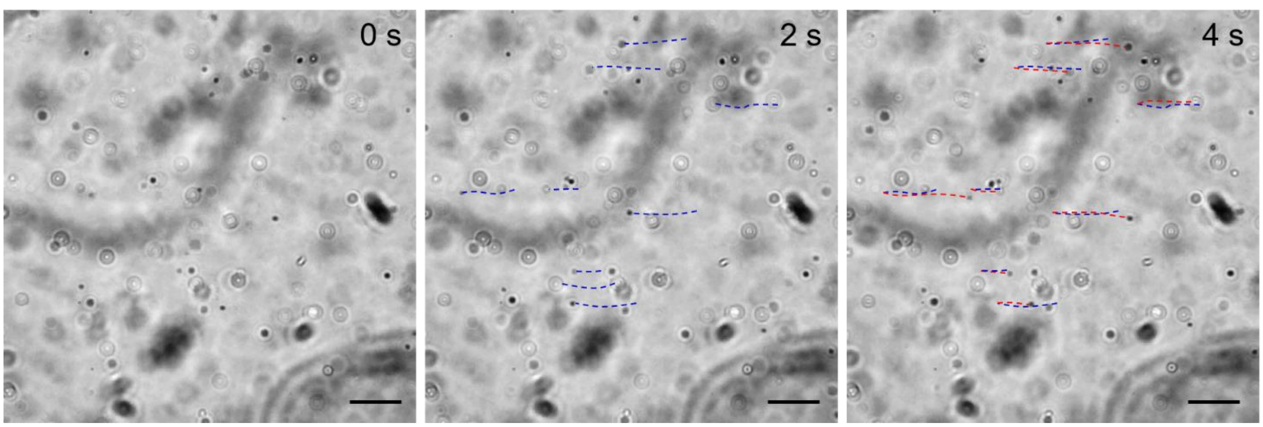

Fig. S4. Time-lapse images showing the controlled movement (forward/backward) of the slippery Fe-containing propellers when actuated by the external magnetic field. The blue dashed lines are the forward moving trajectories and the red dashed lines are the backward moving trajectories. Scale bar 20 μm.

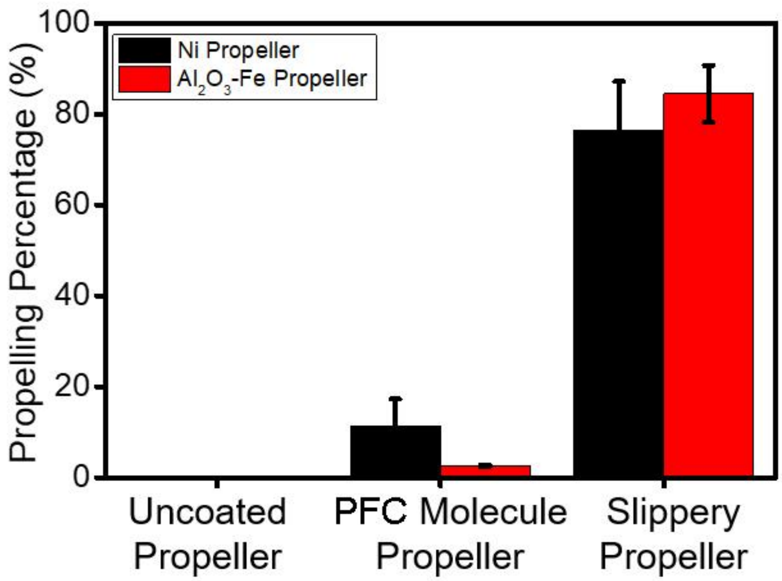

Fig. S5. Percentage of propelling micropropellers containing Ni (black) and those made with Fe (red) in vitreous with different surface coatings. The Fe propellers have been coated with a thin layer (atomic layer deposition) of Al_2O_3 to prevent corrosion. Only when the propellers contain the slippery coating do they move and the Fe propellers show very similar propulsion properties compared with the Ni propellers.

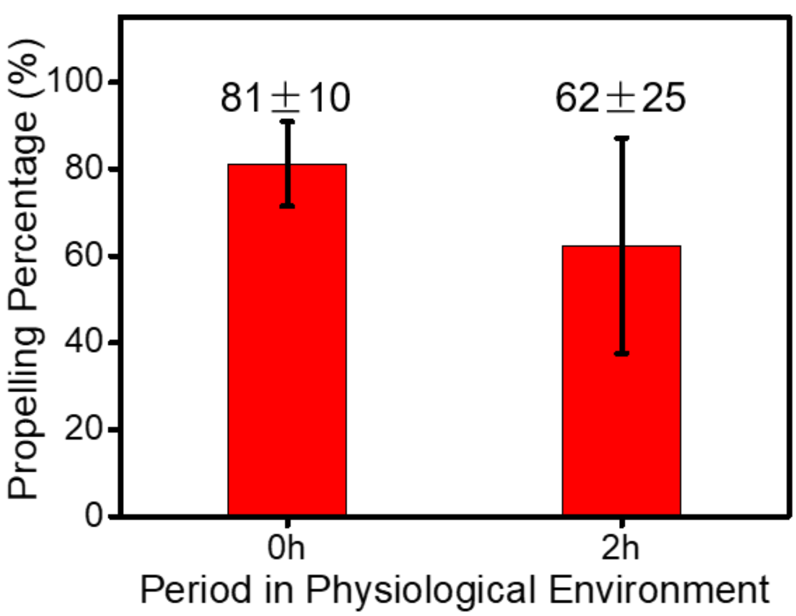

Fig. S6. Percentage of propelling slippery propellers in vitreous before and after incubation within 5% bovine serum albumin in PBS solution for 2 hours.

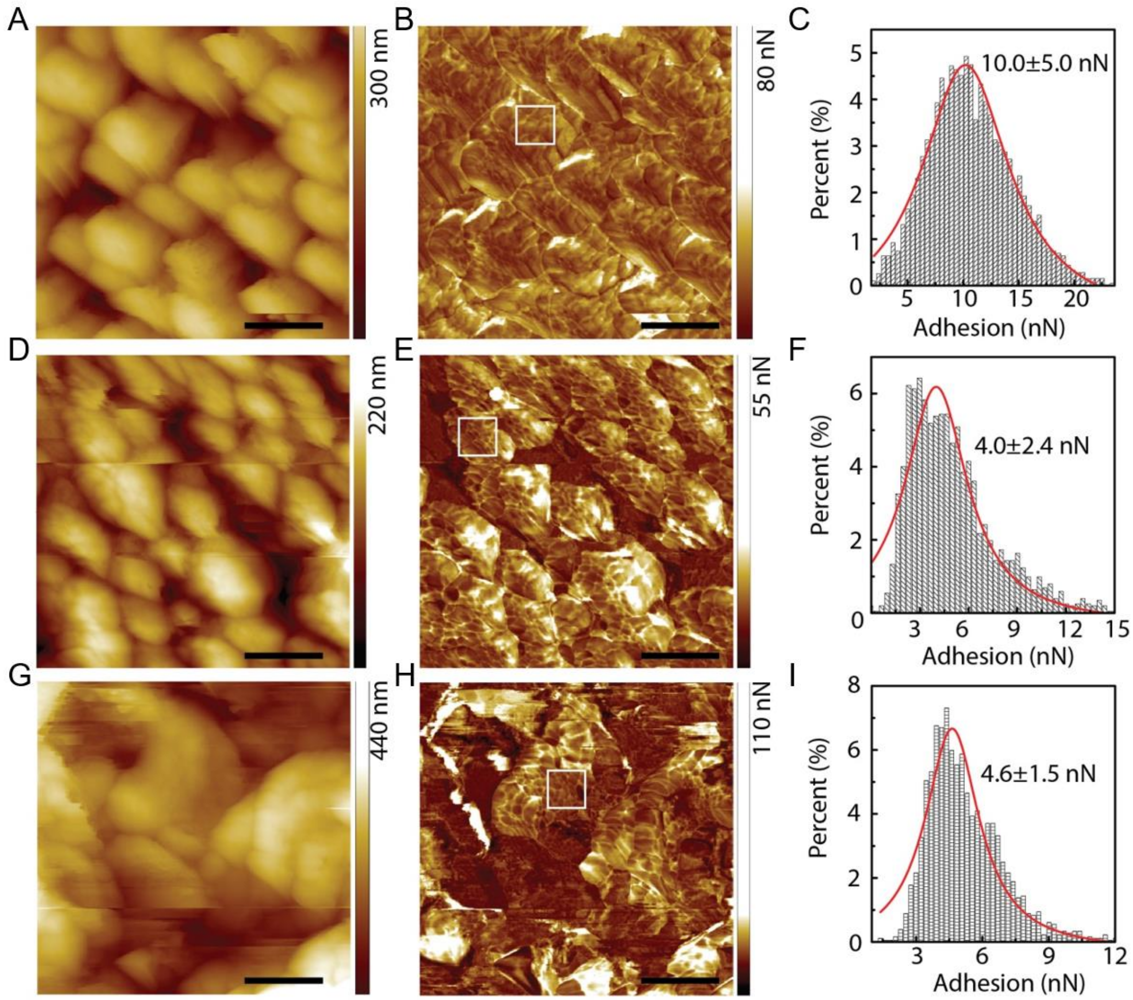

Fig. S7. Characterization of the surface coating on the micropropellers by AFM. The morphology (**A**, **D**, and **G**), the adhesion force (**B**, **E**, and **H**), and the adhesion histograms from the selected areas in B, E, and H (B, **F**, and **I**) of the bare micropropeller without surface coating (A, B, and **C**), the slippery micropropeller with the perfluorocarbon coating (D, E, and F), and the slippery micropropellers with coating and shaken in BSA solution at 37 ºC for 2 h as a mimic of physiological environment (G, H, and I). The results show that the perfluorocarbon coating on the micropropellers lowers the adhesion force (surface energy), and there is no significant change to the properties of the surface coating surface under physiological environment for 2 h. Scale bars 500 nm.

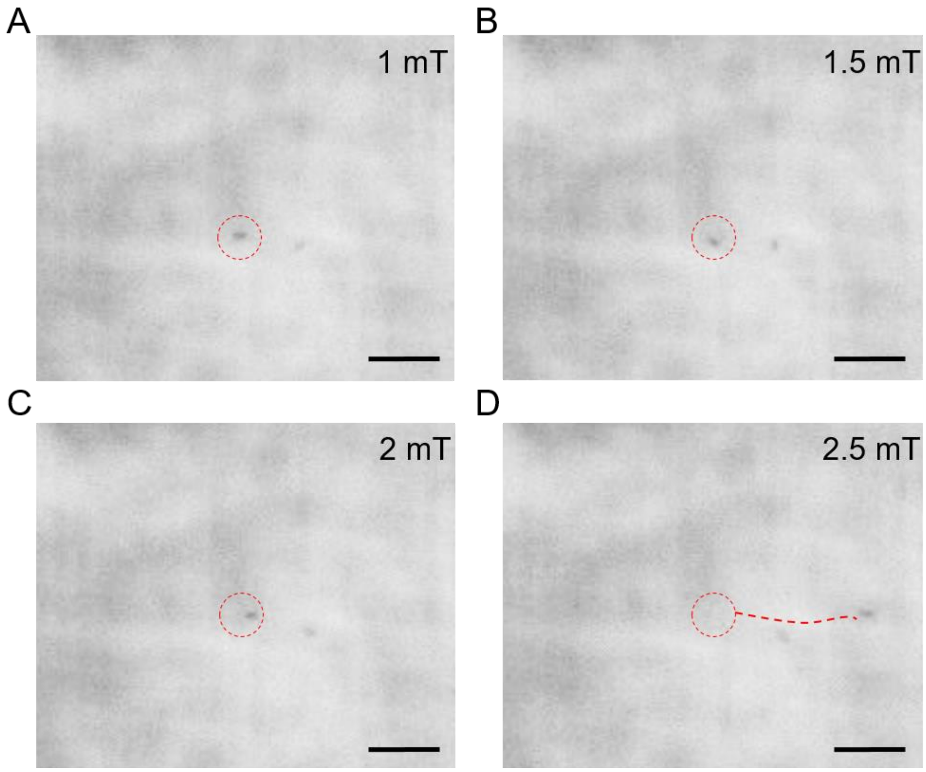

Fig. S8. Intravitreal propulsion of the slippery propellers as a function of the magnetic field strength. 1 mT (**A**), 1.5 mT (**B**), 2 mT (**C**), and 2.5 mT (**D**). Scale bar 10 μm.

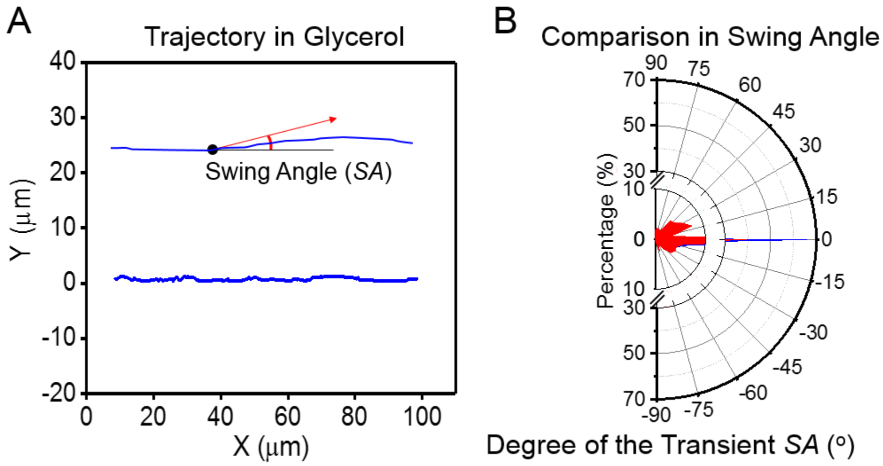

Fig. S9. Propulsion of the slippery micropropellers in glycerol solution. (**A**) Trajectory of the slippery micropropeller in 25% glycerol solution. (**B**) The comparison of the transient swing angle (*SA*) for the movement of the slippery micropropellers in the vitreous (red) and in 25 % glycerol solution (blue).

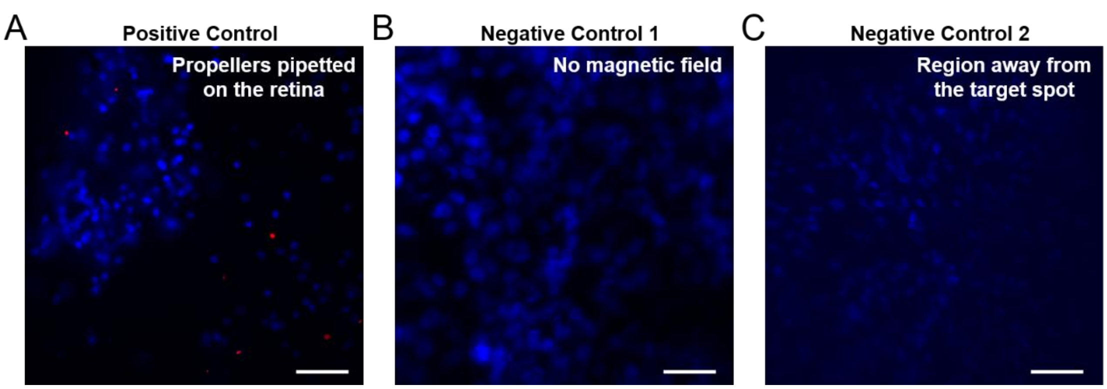

Fig. S10. Fluorescence images of the excised retina. (**A**) The droplets containing fluorescent micropropellers were dropped directly on the retina, as a positive control group. (**B**) Negative control group 1: fluorescent micropropellers were injected into the eye, but no magnetic field was applied. No red fluorescent particles are observed on the retina. (**C**) Negative control group 2: the region of the retina away from the target region (at least 0.5 cm distance from the optic disc) after the swarm of slippery micropropellers was moved through the eye by magnetic propulsion. No red fluorescent particles are observed on the retina away from the optic disk. Scale bars, 20 μm.

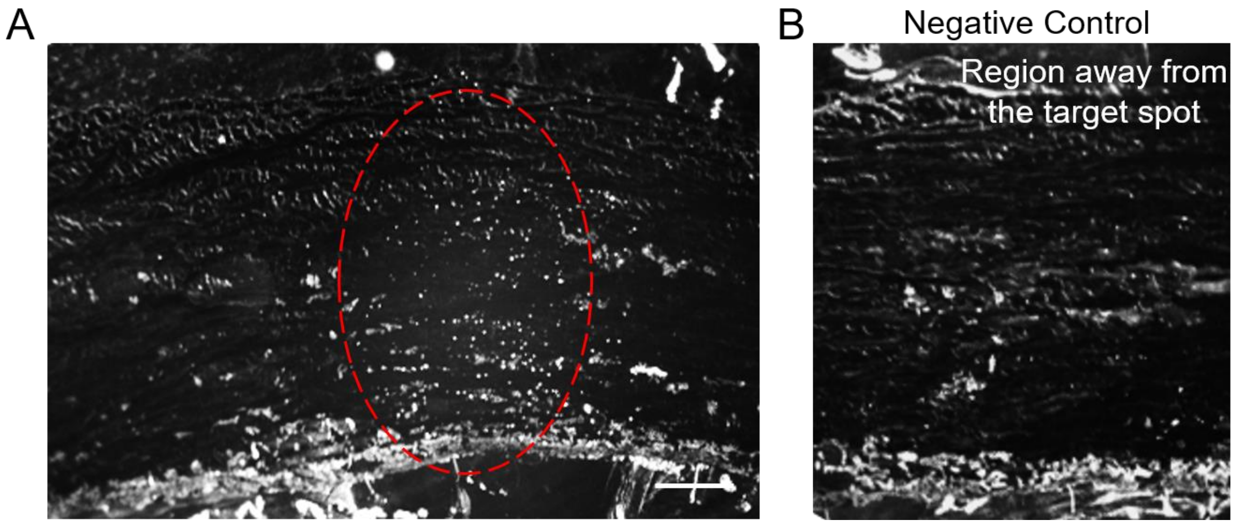

Fig. S11. Investigation of the distribution of the propellers on the retina. Dark field microscope images of the histology near the optic disc (**A**), and the area away from the optic disc as a negative control (**B**). The eye was fixed with glutaraldehyde, and cut it into slices each 13 µm thick. Scale bar 200 µm.

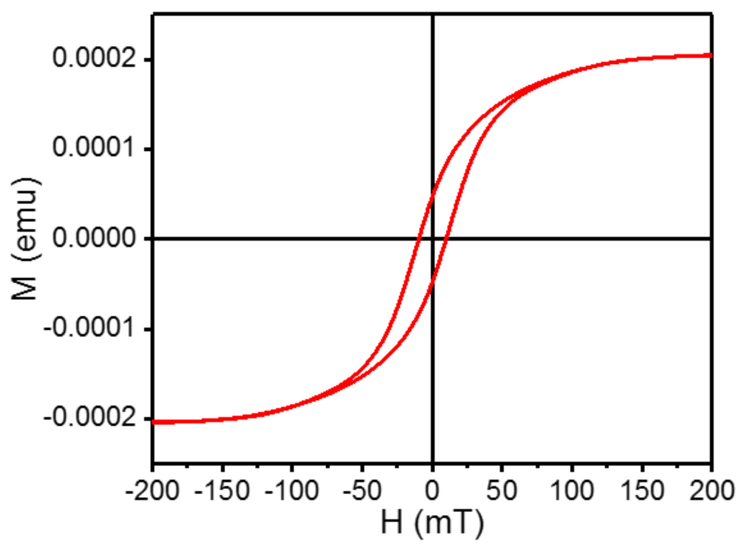

Fig. S12. The M-H curve of a wafer piece (area of 10 mm^2) containing an array of microhelices.

Table S1. Statistical analysis of micropropellers moving in vitreous as a function of the surface coating.

Surface coating	Average propelling percentage	Standard deviation	Total number of counted particles
Bare	0%	0%	150
Bare+ALD	0%	0%	105
PFC molecule	10%	7%	165
PFC molecule+liquid	81%	10%	144
PFC molecule+liquid, physiological environment for 2 h	62%	25%	107

ALD: atomic layer deposition, PFC: perfluorocarbons

Movie S1. Wobbling motion of an uncoated micropropeller in the vitreous under the actuation of a rotating magnetic field with a strength of 8 mT and a frequency of 6 Hz. The movie is slowed down 6 times. Scale bar, 2 μm.

Movie S2. Propulsion of a slippery micropropeller in the vitreous under the actuation of a rotating magnetic field with a strength of 8 mT and a frequency of 6 Hz. The movie is slowed down 6 times. Scale bar, 2 μm.

Movie S3. A large swarm of slippery micropropellers moves across the boundary of an aqueous buffer into the vitreous and continues propelling in the vitreous under a rotating magnetic field with a strength of 8 mT and a frequency of 70 Hz. Scale bar, 20 μm.

Movie S4. Controlled motion of slippery micropropellers in the vitreous under a rotating magnetic field with a strength of 8 mT and a frequency of 50 Hz. The propulsion direction is controlled by changing the direction of the rotational axis of the external magnetic field. Scale bar, 10 μm.

Movie S5. OCT shows the distribution of the slippery micropropellers at the vitreous-retina boundary. The slippery micropropellers were injected into the center of the porcine eye and propelled by the external rotating magnetic field (a strength of 8 mT and a frequency of 70 Hz for 1 h). The movie displays a sequence of OCT images at different scanning planes at 5 frames/s.